Plasma Propulsion

LABORATORY

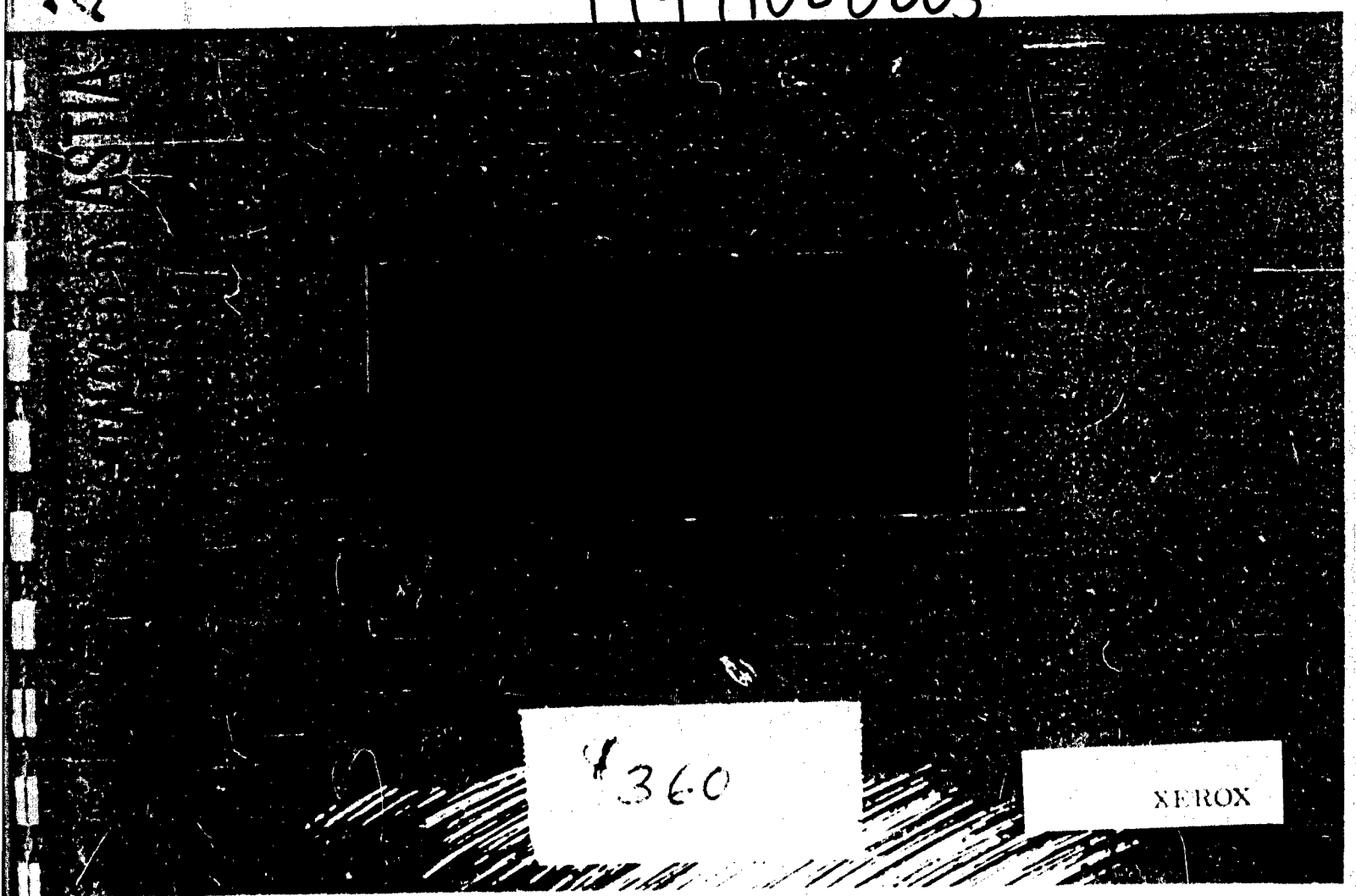

REPUBLIC AVIATION CORPORATION FARMINGDALE NEW YORK

PPL-TR-60-17

ANALYSIS OF THRUST MEASURING DEVICES FOR PULSE SYSTEMS

by

Melvin Zaid

Technik Incorporated
600 Old Country Road
Garden City, N. Y.

for

Plasma Propulsion Laboratory
Republic Aviation Corporation
Farmingdale, New York

Plasma Propulsion Laboratory
REPUBLIC AVIATION CORPORATION
Farmingdale, New York

November, 1960

CONTENTS

I - INTRODUCTION

A - Statement of Problem

The problem is to measure the thrust output of a rocket engine. During the test run, the engine is contained in a vacuum chamber as shown in Figure 1.

FIG. 1

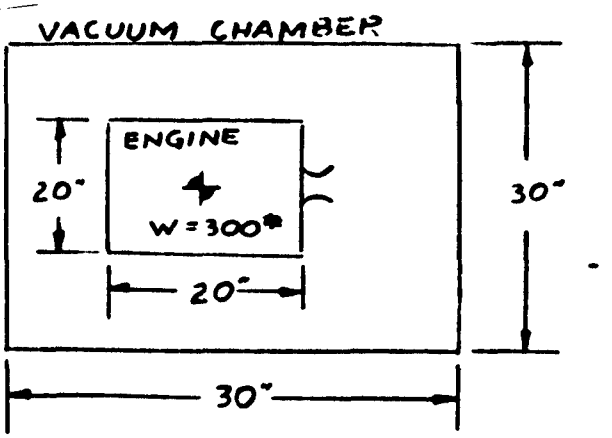

The thrust output consists of a series of short pulses as shown in Figure 2.

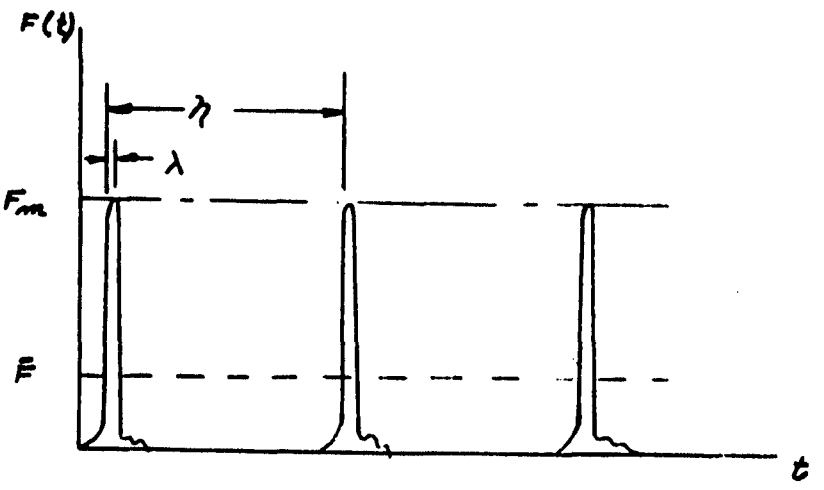

FIG. 2

The thrust specifications are, approximately:

$$F_m = 20 \text{ pounds}$$

$$\lambda = .5 \times 10^{-3} \text{ seconds}$$

$$.10 \leq \eta \leq 2 \text{ seconds}$$

$$.10^{\#} \geq \bar{F} \geq .005 \text{ pounds}$$

where $\bar{F}$ is an "equivalent" average force defined by equating the actual impulse to the equivalent impulse; i.e. $\bar{F}\eta = \int_0^{\lambda} F dt \approx F_m \lambda$

B - General Equations

Consider an idealized free-body diagram of the engine as shown in Figure 3.

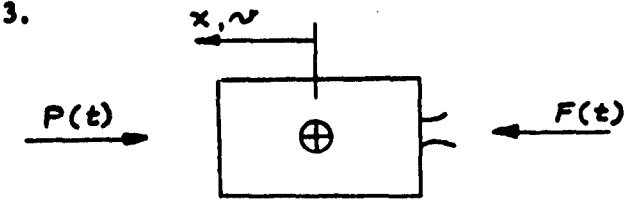

FIG. 3

The equation of linear momentum in the horizontal direction may be written as:

$$\int F(t)dt - \int P(t)dt = \Delta(mV)_{\substack{rigid \\ body}} + \Delta(mV)_{internal} \qquad (1)$$

where the left side is the net impulse applied to the engine and the right side is the total change of momentum. The total change of momentum is considered to have two components:

1. $\Delta (mV)_{\text{rigid body}}$ = the momentum change considering the entire mass of the engine moving as a rigid body.

2. $\Delta (mV)_{\text{internal}}$ = the change in the relative momentum of internal moving or vibrating elements where their momentum is taken relative to the rigid body motion.

When the engine is used to drive a vehicle in space, the useful momentum imparted to the vehicle is just the first of the above two components. It is desired to obtain an indication of this momentum by means of a laboratory measurement; in which it will be possible to measure $P(t)$ and $\Delta (mV)_{\text{rigid body}}$ experimentally. Rewriting equation (1) with the subscript "L" referring to laboratory conditions, and "S" to space conditions, we have:

$$\int F_L(t)dt - \int P_L(t)dt = \Delta(mV)_{\substack{\text{rigid} \\ \text{body,L}}} + \Delta(mV)_{\text{internal}_L} \quad (2)$$

$$\int F_S(t)dt - \int P_S(t)dt = \Delta(mV)_{\substack{\text{rigid} \\ \text{body,S}}} + \Delta(mV)_{\text{internal}_S} \quad (3)$$

Now consider that the resistance in space is zero ($P_s(t) = 0$), and that the engine is mounted in the laboratory so that $\Delta(mV)_{internal_L} = \Delta(mV)_{internal_S}$ and that the engines behavior (or its equivalent) is essentially the same in the laboratory or in space so that

$$\int F_S(t)dt = \int F_L(t)dt$$

then, substituting the above into equations (2) and (3) and eliminating the engine impulse term, we have

$$\int P_L(t)dt + \Delta(mV)_{\substack{rigid \\ body,L}} = \Delta(mV)_{\substack{rigid \\ body,S}} = \int F(t)dt_{useful} \quad (4)$$

Hence, the laboratory measurement gives a direct indication of the useful momentum generated by the engine in space.

The internal momentum may consist of a vibration of internal components relative to the frame. Whether or not this vibration affects the measurements to be made, remains to be experimentally determined; but this effect can be made negligibly small by careful design techniques.

C - General Systems

The problem resolves itself to the instrumentation and measurement of the left side of equation (4); three general approaches are possible. For our initial purposes of discussion, they are presented in ideal schematic form; the engine is taken to be resting on a frictionless surface and translates due to the thrust impulses. It is noted, however, that torsional

analogies exist for these cases which may be more practicable.

1. Infinitely-Rigid System

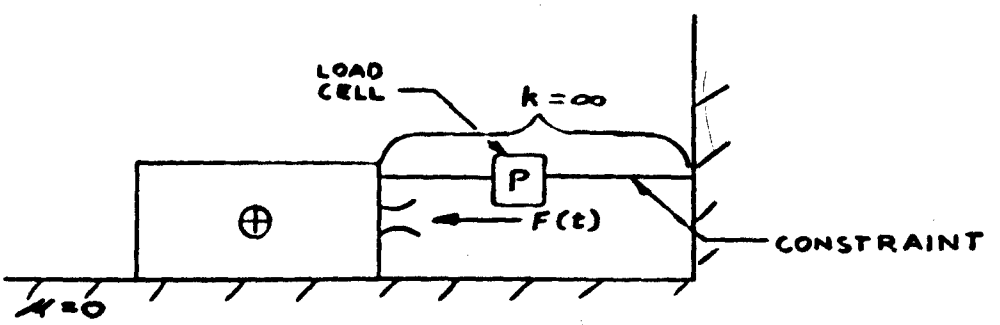

FIG. 5

In the above figure, the engine is resting on a frictionless surface. It is essentially restrained from motion so that $\Delta(mv) = 0$, and from equation (4), the impulse induced in the load cell equals the useful thrust impulse:

$$\int P_L(t)\,dt = \int F_{useful}(t)\,dt \qquad (5)$$

Furthermore, since $\Delta(mv) \approx 0$ at all times during the impulse equation (5) holds at any generic time during the impulse; which leads to,

$$P(t) = F(t) \qquad (6)$$

Thus, for an ideally rigid system, the instantaneous force in the load cell equals the instantaneous value of thrusts as shown in the following figure:

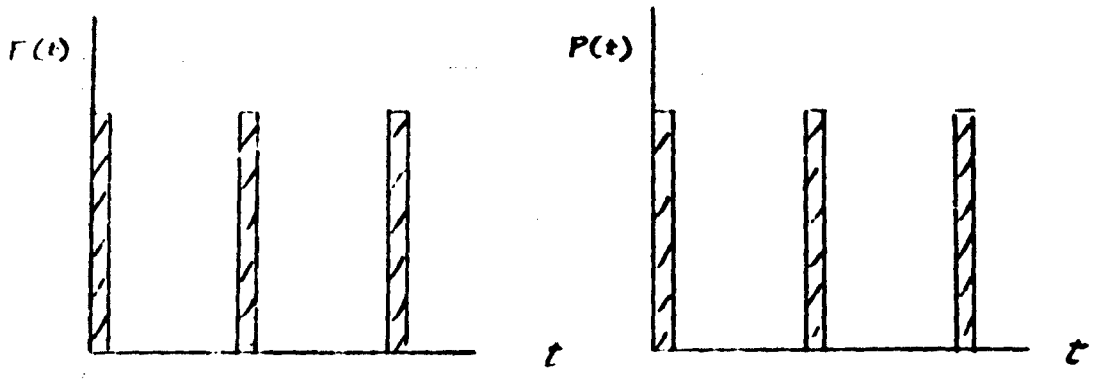

FIG. 6

To determine the feasibility of this system, we must consider how closely a real system may approximate the ideal. The duration of a thrust pulse is 0.5 milliseconds; the minimum spacing between pulses is 100 milliseconds. Thus, we consider the response of the system to an individual pulse. It can be shown that for the system to adequately track a rectangular pulse, its natural frequency must be at least as high as the frequency associated with the individual pulse duration. In this system, this means that the natural frequency of the engine-restraining rod must be at least 1000 cps. Taking the engine weight at 300 pounds, the spring constant of the restraining rod is calculated to be about 40×10^6 pounds/inch. Considering a rod of length ℓ, we have

$$k = \frac{P}{\delta} \quad ; \quad \epsilon = \frac{\delta}{\ell}$$

so that

$$\epsilon = \frac{P}{k\ell}$$

For a peak pulse of 20#, and an effective length of .1" (the shortest feasible strain gage length) we have

$$\varepsilon \sim 5 \times 10^{-6} \ in/in$$

which is just at the border for "state-of-the-art" techniques.

2. Infinitely-Flexible System

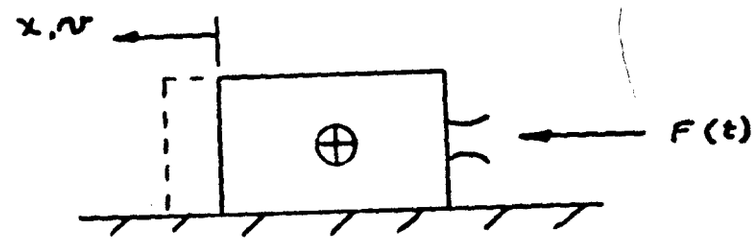

FIG. 7

Here, the engine is idealized to be free of all external forces, so that from equation (4)

$$\Delta (mV)_{\substack{rigid \\ body, L}} = \int_{useful} F(t)\,dt \qquad (7)$$

Considering one pulse:

$$\int F(t)dt \approx F_m \lambda = 20 \times .0005 = .010 \ \frac{\#\,sec}{Pulse} \qquad (8)$$

then, since m is constant:

$$\Delta V = \frac{1}{m} F_m \lambda = \frac{1}{\frac{300}{386}} \times .010 = .013 \ \frac{in/sec}{Pulse} \qquad (9)$$

If the engine is initially at rest, the velocity after the "n^{th}" pulse will be:

$$V(n) = n\Delta V = .013n \quad in/sec \qquad (10)$$

The velocity after 10 pulses will be:

$$V(10) = .13 \quad in/sec$$

which is easily measured. The distance moved depends on the spacing between pulses. In the case of 2 second spacing, the distance moved during 10 pulses (i.e. 20 seconds) is about:

$$x \approx \frac{.13}{2} x20 = 1.3 \quad inches \qquad (11)$$

Hence, if the pulse spacing is known, it may be more practicable to measure displacement and, by calculation, determine the momentum change and thrust. Whichever is instrumented and measured, it is seen that the measurements are well within the range of feasibility. Thus, this system is, in principle, feasible.

The next step is to consider reducing this system to practice. The problem is to provide a near-frictionless sliding surface. For reasonable accuracy of measurement, the friction force should be no more than one-tenth of the minimum average thrust value. From Figure 2, the average thrust has a minimum value of 0.005 pounds.

Thus, the friction force should be of the order of 0.0005 pounds; which implies a coefficient of friction of:

$$f \leq \frac{.0005}{300} \sim 2 \times 10^{-6} \qquad (12)$$

This friction factor is so small as to exclude any system based on solid-to-solid sliding or rolling contact. Three approaches based on fluid film lubrication are as follows:

a. Oil film bearing: With the present state-of-the-art, it is possible to obtain friction factors in the order of 10^{-4}. While it may be possible to improve this value with a very sophisticated design, this direction does not seem to be promising.

b. Air film bearing: A good bearing design may result in a friction factor of the order of 10^{-6}. However since the engine test chamber is evacuated this leads to two problems. The first, maintaining an air film in a vacuum, may be difficult to achieve. The second, the efflux of air from the bearing will put additional strain on the vaccum pumps working with the test chamber. Although this approach has problems associated with it, it merits further study.

c. Mercury bath flotations: In this approach, the entire engine is floated in a bath of mercury as shown in figure 8.

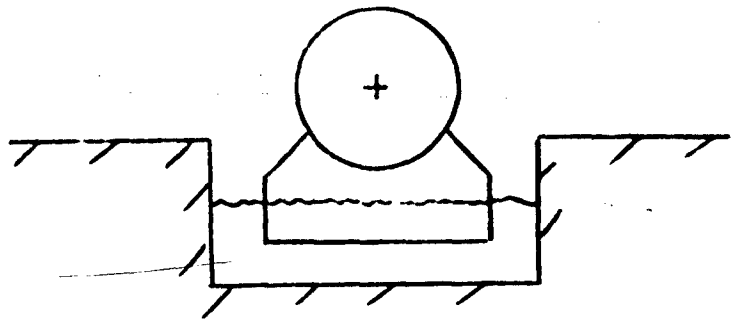

FIG. 8

With proper design, it seems likely that the friction can be reduced to very low values. The detailed design, with consideration of friction, overturning stability, effects of waves, quantity of mercury required, etc. is beyond the scope of this report.

3. Intermediate-Stiffness System

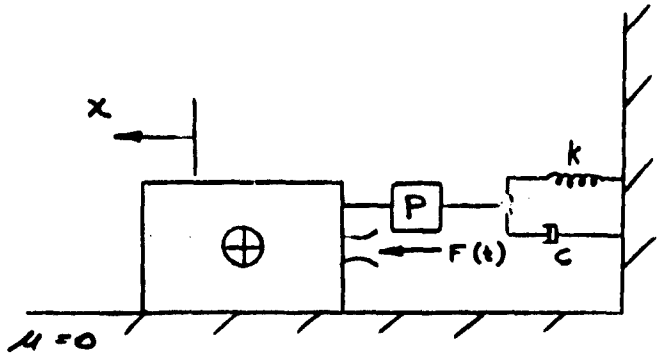

FIG. 9

In this system, the engine is coupled to the ground by a spring and dashpot. The equation of motion is:

$$\frac{W}{g}\ddot{x} = F(t) - kx - c\dot{x} \qquad (13)$$

which may be rewritten in standard form as:

$$\ddot{x} + 2\mu\dot{x} + \omega^2 x = \frac{g}{W} F(t) \qquad (14)$$

where

$$2\mu = \frac{cg}{W} \; ; \qquad \omega^2 = \frac{kg}{W} \qquad (15)$$

It is recalled that $F(t)$ represents a series of pulses whose spacing may vary from 2 seconds to 0.10 second. The form of the solution to equation (14) depends on the relation between the period of natural vibration of the engine-spring-dashpot system and the inter-pulse period.

If the period of natural vibration is short compared to the inter-pulse period, then the response of this system will approach that of the infinitely-stiff system considered in section 1. Whereas, if the period of natural vibration is long compared to the inter-pulse period, then the response of this system approaches that of the infinitely soft system considered in section 2. In between these extremes we have the soft or stiff systems, which are described in more detail in Part III of this report. However, we will state the one essential characteristic that differentiates them from each other. The soft system basically integrates the pulses until a steady state position is attained; so that it can only be expected to work well if the inputs are essentially non-varying in amplitude or spacing

and if enough time is allowable for steady conditions to be reached. On the other hand the stiff system measures each pulse as it occurs. Thus since it essentially responds to transient phenomena it can tolerate non-steady or short time phenomena (even single pulse inputs).

II - INTERMEDIATE STIFFNESS SYSTEMS - DETAILED INVESTIGATIONS

A - Soft System

1. Introduction

Various mechanizations exist in this general class. Among these are the seismic pendulum previously proposed and the inverted pendulum system under current consideration. Although we treat the inverted pendulum in detail here, much of the general results apply equally well to the seismic pendulum. The inverted penulum system is based on the torsional analog of Figure 9 for the case of a very flexible system. Schematically, it is shown in Figure 10 below:

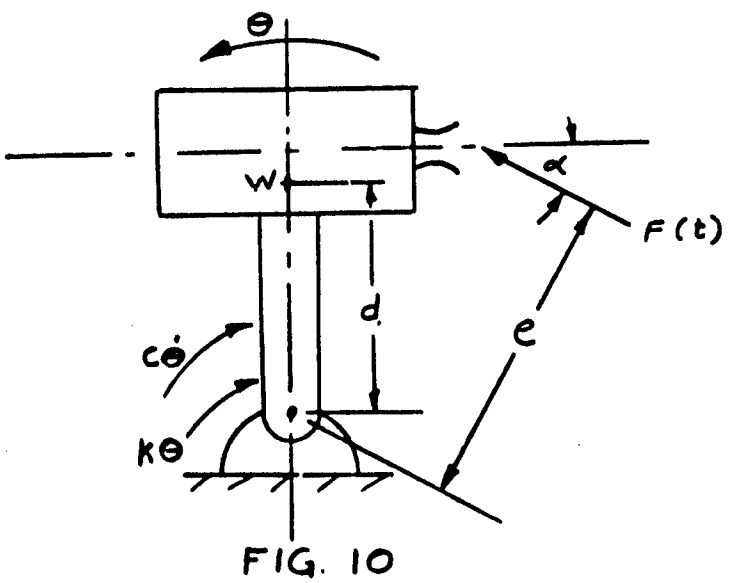

FIG. 10

The pivot is assumed to be ideal and frictionless. In the actual system, the pivot will be provided by a non-slipping torsional restoring spring. Because of the absence of relative slipping motion between elements, the friction torque may be almost negligible; consisting of internal hysteresis of the material itself.

2. Static Analysis

As seen in Figure 2, $F(t)$ may be considered to have an average value $\bar{F}$. As an introduction, let us consider the steady-state deflection of this system under an applied constant force $\bar{F}$; i.e., at times great enough for all transient effects due to initial application of this force $(\bar{F})$ to be damped out.

From statics:

$$\bar{F}e + Wd \sin\theta_s = k\theta_s \qquad (16)$$

where θ_s = steady-state deflection of the system. If θ_s does not exceed about 5 or 6 degrees, $\sin\theta_s$, may be approximated by θ_s. Hence:

$$\bar{F}e + Wd\,\theta_s = k\theta_s \qquad (17)$$

or

$$\theta_s = \frac{\bar{F}e}{k - Wd} \qquad (18)$$

Equation (18) shows that the static sensitivity may be increased by decreasing the effective spring constant $k - Wd$. Let us, for example, set the sensitivity so that the maximum value of $\bar{F}$ (0.100 pounds)

causes a deflection (θ_s) of 0.10 radians (5.73°). Taking " d " and " e " to be about 10 inches, we find:

$$k - Wd = \frac{\bar{F}e}{\theta_s} = \frac{.100 \times 10}{.1} = 10 \ \frac{in\#}{rad.} \quad (19)$$

while for W = 300 pounds:

$$k = \frac{\bar{F}e}{\theta_s} + Wd = 10 + 300 \times 10 = 3010 \ \frac{in\#}{rad.} \quad (20)$$

Thus, to get accurate results, the calibration must set the difference between k and Wd to a value which is a small difference of large numbers and maintain that calibration within close tolerances throughout the entire test. This is generally a problem and may be expected to be troublesome.

The problem of maintenance of calibrations is an important one and any specific design must be carefully evaluated and experimentally verified before and after each test to ascertain the constancy of $k - Wd$ to within very close tolerances. Otherwise θ_s will not remain constant but will fluctuate so that the test is difficult to interpret. Assuming that the design is adequate, it is simpler to adjust and calibrate the system. If it is noticed that ($k - Wd$) is the effective spring constant for the system and, hence, determines the undamped natural frequency, a very effective method of calibration results. The undamped natural vibration will have a period:

$$T = 2\pi \sqrt{\frac{I_o}{k - Wd}} \quad seconds \quad (21)$$

where I_o is the mass moment of inertia about the pivot. To estimate this, we have

$$I_o = I_{c.g.} + \frac{W}{g} d^2 = \frac{1}{12} \frac{W}{g} L^2 + \frac{W}{g} d^2 \qquad (22)$$

where the moment of inertia of a uniform cylinder of length L was taken for I_g. Taking L as 20 inches, we have:

$$I_o = \frac{1}{12} \times \frac{300}{386} \times (20)^2 + \frac{300}{386} (10)^2 \approx 100 \quad \#\,in\,sec^2 \qquad (23)$$

Using this value in equation (21)

$$T = 2\pi \sqrt{\frac{100}{10}} \approx 20 \ sec. \qquad (24)$$

Thus, having selected a sensitivity of .10 radians for .100 pounds average thrust, the period of undamped vibration is 20 seconds. Further, since $\frac{I}{k - wd} \propto T^2$ this provides an experimental method of checking the calibration which should be quite accurate.

Let us examine the previous selected sensitivity to establish its accuracy. Let δ_s be the displacement at the c.g. associated with θ_s ; hence $\delta_s = \theta_s d$. Now,

$$\frac{\delta_s}{F} = \frac{\theta_s d}{F} = \frac{.10 \times 10}{.100} = 10 \ ^{in}/_{\#} = .010 \ ^{in}/_{.001\#} \qquad (25)$$

Thus, since a .010 inch deflection may be measured with reasonable accuracy, we see that this system can measure the average thrust within .001 pounds.

In the following section, we will take the sensitivity, effective spring constant and natural period of vibration at the same value used in this example.

3. Dynamic Analysis

From Figure 10, the dynamic equation of motion is:

$$\ddot{\theta} + 2\mu\dot{\theta} + \omega^2\theta = \frac{e}{I_o}F(t) \qquad (26)$$

where

$$2\mu = \frac{c}{I_o} \quad ; \quad \omega^2 = \frac{k - Wd}{I_o} \qquad (27)$$

Case I - Quasi-static

Since the natural period of pendulum vibration is of the order of 20 seconds and the pulse spacing is about 1 or 2 seconds, it would be expected that the response of the pendulum would be primarily determined by the average value of $F(t)$. In the preceding section, we considered the steady-state effect of a constant thrust, here we consider the transient effect which, with the passing of time, approaches the steady-state. In this we will idealize the pendulum so that all variations in physical parameters or non-ideal motions are excluded; although they may actually cause additional non-negligible deviations from the motions described below.

Letting $F(t)=\bar{F}$ the solution of equation (26) is:

$$\theta(t)=e^{-\mu t}\left(A\cos\sqrt{\omega^2-\mu^2}\,t+B\sin\sqrt{\omega^2-\mu^2}\,t\right)+\frac{\bar{F}e}{\omega^2 I_o} \qquad (28)$$

Taking the system initially at rest, we find:

$$\theta(t)=\theta_s\left[1-\frac{\omega}{\sqrt{\omega^2-\mu^2}}e^{-\mu t}\cos\left(\sqrt{\omega^2-\mu^2}\,t-\tan^{-1}\frac{\mu}{\sqrt{\omega^2-\mu^2}}\right)\right] \qquad (29)$$

where:

$$\theta_s=\frac{\bar{F}e}{\omega^2 I_o}=\frac{\bar{F}e}{k-Wd} \qquad (30)$$

and is the same value as in equations (18). It is seen from equation (29) that as time increases, the transient oscillations are damped out and the displacement $\theta(t)$ approaches the steady-state displacement θ_s

To get a quantitative picture of the transient oscillations, and the effects of damping, let us evaluate equation (29) for the same physical parameters selected previously. Hence, let:

I_o = 100 pound inches

e = 10 inches

d = 10 inches

$k-Wd$ = 10 inch pounds/radian

T = 20 seconds or $\omega=\frac{2\pi}{T}=.314\ \frac{rad}{sec}$

Now, equation (28) is the solution of equation (26) only if μ is less than

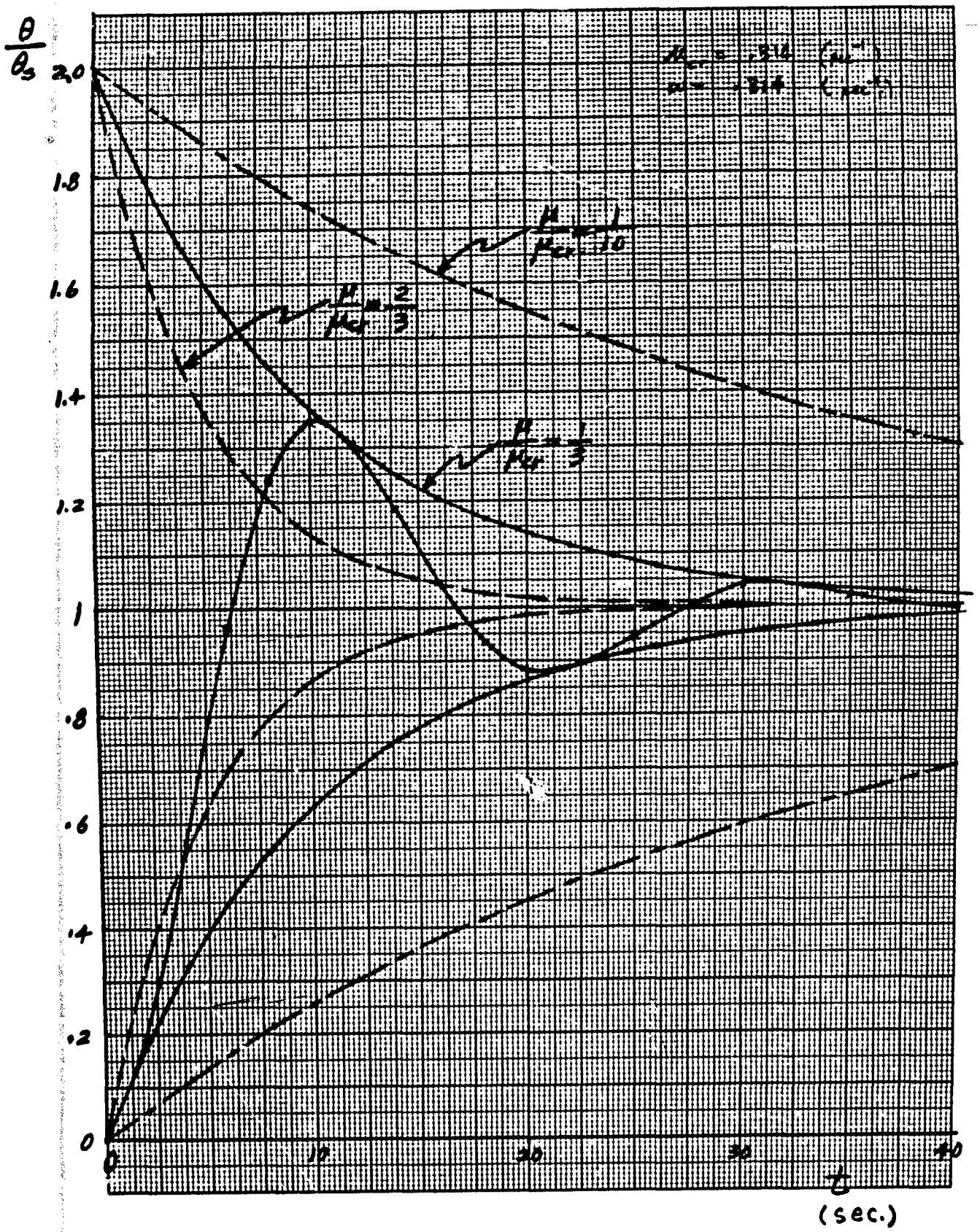
θ/θs
2.0
1.8
1.6
1.4
1.2
1
.8
.6
.4
.2
0
0
10
20
30
40
t
(sec.)
μ/μcr = 1/10
μ/μcr = 2/3
μ/μcr = 1/3

FIG. 11

If μ equals, or is greater than, ω, the solution of equation (26) is not a damped oscillation but an asymptotic approach to θ_s. Hence, let us define μ_{cr} as the value of μ which is equal to ω; i.e.:

$$\mu_{cr} = \omega \qquad (31)$$

Using the above values together with equation (30), the envelope of equation (29) is plotted for several values of damping; see Figure 11. Here the displacement is in the dimensionless form of θ/θ_s; since $\bar{F}$ affects only θ_s, these curves are valid for all values of $\bar{F}$. To aid clarity, the oscillatory motion is shown only for one value of damping. For the other values of damping, the curves will be of the same form but bounded by their respective damped exponential envelopes.

Experimentally, it is desired to measure θ_s to be able to determine the average thrust $\bar{F}$. However, it is seen that damping determines how soon the transient oscillations decay and the displacement settles down to its steady-state value. If we define the displacement error (ε) as the maximum deviation of θ from θ_s, using equation (29) we find:

$$\varepsilon = \pm e^{-\mu t} \theta_s \qquad (32)$$

which decays to zero as time increases. For t = 20 seconds, equation (32) may be evaluated to give,

$\frac{\mu}{\mu_{cr}}$	μ	$e^{-\mu t}$	ε
.10	.0314	.550	$.550\theta_s$
.33	.1050	.140	$.140\,\theta_s$
.67	.2100	.015	$.015\,\theta_s$

Thus, for a test reading after 20 seconds, it is seen that the damping must be in order of one-half critical for the displacement error to be below ten percent.

Case II - Periodic Thrust Pulses

We now consider equation (26) for the case where $F(t)$ consists of a periodic series of pulses as shown in Figure 2. Since $\lambda << \eta$ we approximate each pulse with a dirac-function pulse having the same impulse (i.e. area on $F-t$ graph); see Figure 12.

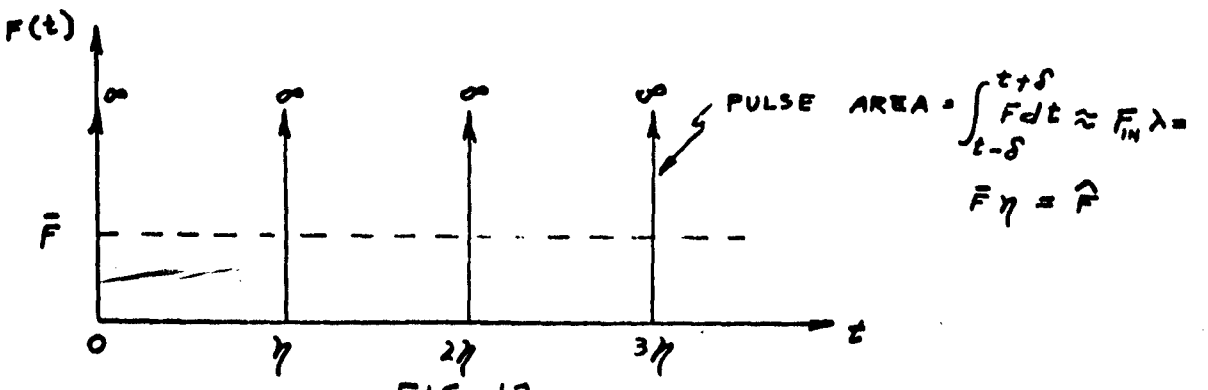

FIG. 12

Since the area under a " δ " -pulse is unity, we may write:

$$F(t) = \hat{F}\left[\delta(0) + \delta(\tau) + \delta(2\tau) + \text{- - - - - - -}\right] \qquad (33)$$

Then, the equation of motion, from equations (26) and (33) is:

$$\ddot{\theta} + 2\mu\dot{\theta} + \omega^2\theta = \frac{e}{I_o}\hat{F}\left[\delta(0) + \delta(\tau) + \delta(2\tau) + \text{- - - -}\right] \qquad (34)$$

Taking the Laplace transform of both sides:

$$\phi(s)\left[s^2 + 2\mu s + \omega^2\right] = \frac{\hat{F}e}{I_o}\left(\frac{1}{1-e^{-\tau s}}\right) \qquad (35)$$

where

$$\phi(s) = \mathcal{L}\left[\theta(t)\right]$$

hence

$$\phi(s) = \frac{\hat{F}e}{I_o}\left(\frac{1}{s^2+2\mu s+\omega^2}\right)\left(\frac{1}{1-e^{-\tau s}}\right) \qquad (36)$$

To obtain $\theta(t)$, we need the inverse transform of equation (36); it is obtained from Table 6.2 of "Advanced Engineering Mathematics" by C.R. Wylie, Jr. Using the appropriate inverse transform the solution to equation (36) may be expressed as:

$$\frac{\theta(t)}{\theta_s} = \frac{\eta\omega^2}{\sqrt{\omega^2-\mu^2}}\left\{ \frac{e^{-\mu\tau}\sin\left[\sqrt{\omega^2-\mu^2}(\tau+\eta)\right] - e^{-\mu(\tau+\eta)}\sin\left[\sqrt{\omega^2-\mu^2}\,\tau\right]}{2\cosh\eta\mu - 2\cos\eta\sqrt{\omega^2-\mu^2}} \right.$$

$$\left. - \frac{e^{-\mu t}\sin\left[\sqrt{\omega^2-\mu^2}(t+\eta)\right] - e^{-\mu(t+\eta)}\sin\left[\sqrt{\omega^2-\mu^2}\,t\right]}{2\cosh\eta\mu - 2\cos\eta\sqrt{\omega^2-\mu^2}} \right\} \quad (37)$$

where

$$0 \le t \le \infty \; ; \quad c\eta < t < (c+1)\eta$$

$$\tau = -(c+1)\eta + t \; ; \quad -\eta \le \tau \le 0$$

$$c = 0,\ 1,\ 2,\ \cdots\cdots$$

and $c\eta$ indicates the time at which the most recent pulse occurs.

Additionally,

$$\theta_s \eta\omega^2 = \frac{\hat{F}e}{I_o} = \frac{\bar{F}\eta e}{I_o}$$

The preceding limits indicate that t and τ are related as shown below:

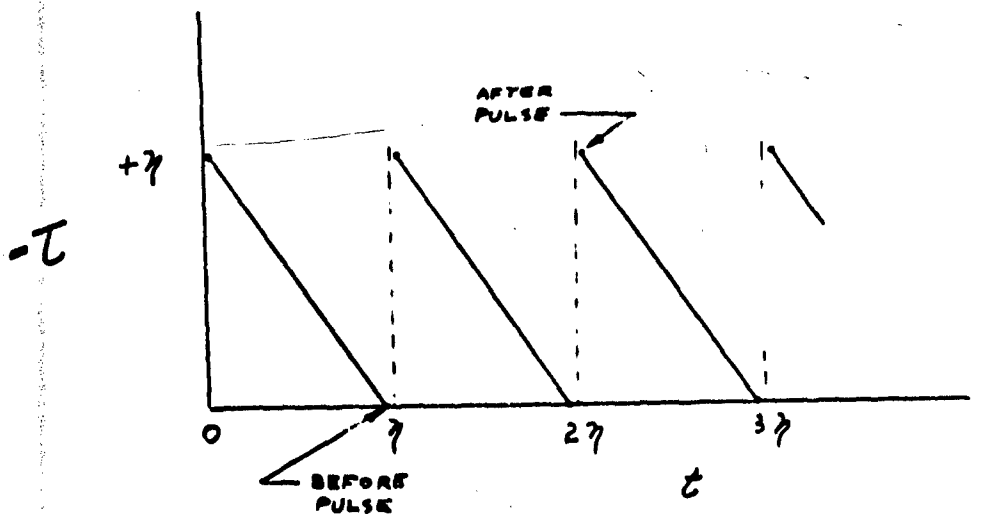

It is seen that the response is composed of two components:

1. a periodic oscillation at the pulse frequency, since $-\eta \leq \tau \leq 0$
2. a damped oscillation at the pendulum frequency, since $0 \leq t \leq \infty$

Hence, we write:

$$\frac{\theta(t)}{\theta_s} = \left(\theta_t(t) + \theta_s\right) + \left(\theta_{ss}(t) - \theta_s\right) \qquad (38)$$

Let us evaluate this solution for the same physical parameters used before and for damping about one-third of critical (i.e., $\mu = .10$). Since the effect due to pulsing increases as the pulse frequency approaches the pendulum frequency, we select the pulse period η at its maximum value of 2 seconds.

Equation (37) has been evaluated for the above values and is plotted in Figure 13 where $(\theta_t + \theta_s)$ and $(\theta_{ss} - \theta_s)$ are plotted separately. For comparison, the quasi-static solution previously obtained is also indicated.

It is seen that the response to the pulsing is essentially the same as to a constant force equal to the average value except for a superimposed oscillation at the pulse frequency.

Case III - Non-periodic Thrust Pulses

In the previous case, it was found that the response to a periodic pulse train is essentially the same as to a constant force. Let us here determine the effect of non-periodicity on the system response.

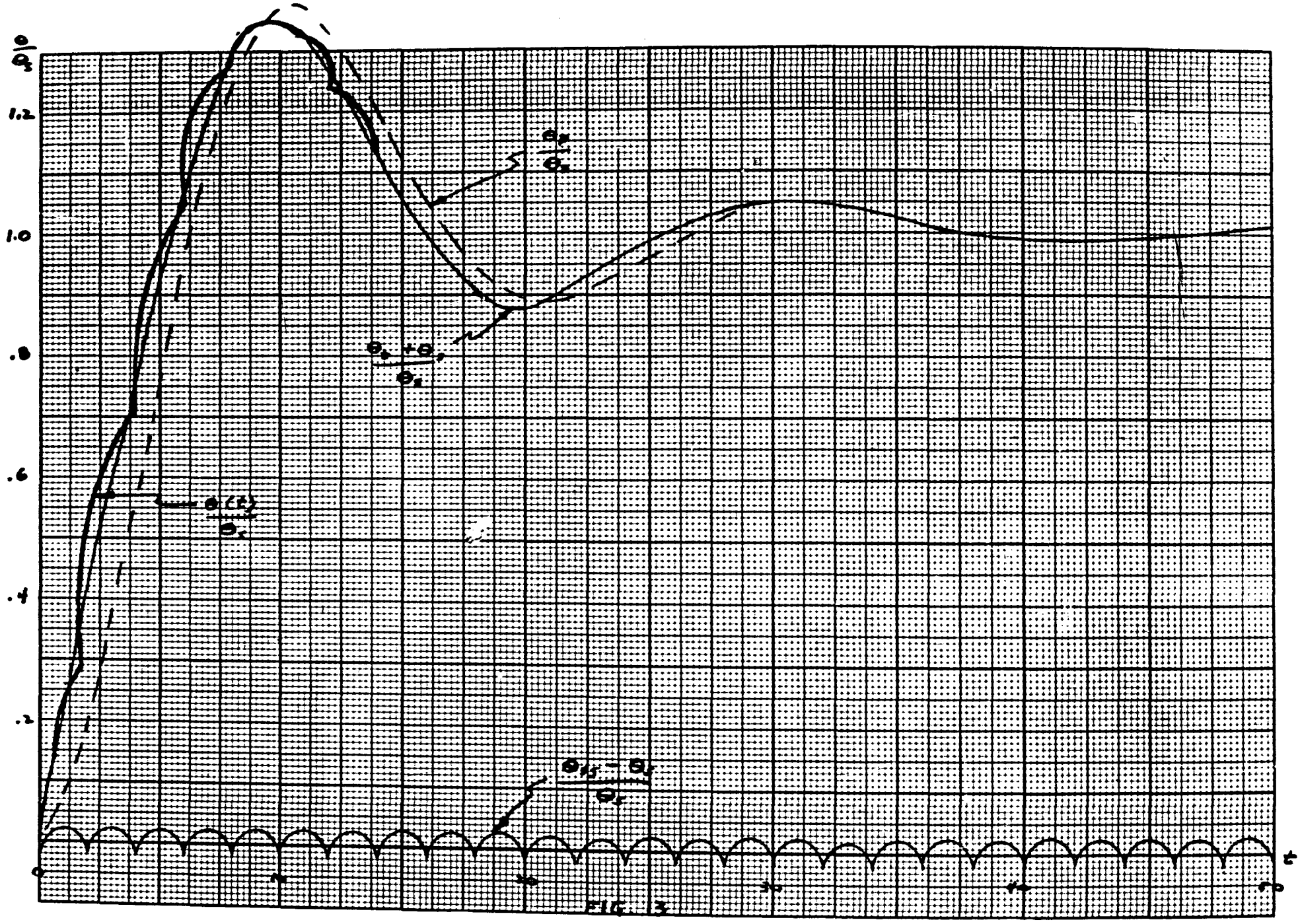

FIG. 3

For non-periodic, $F(t)$, the Laplace transform technique cannot be readily used. Hence, we consider a superposition technique based on the Duhamel Integral as discussed in "Vibration Problems in Engineering" by S. Timoshenko. It is easily shown from this integral that the displacements associated with a single impulse are superposable; if each displacement is measured, in time, from the associated pulse.

The effect of a single impulse, $at\ t=o$, of magnitude $\hat{F}$ may be derived from the above reference to be:

$$\theta_i(t) = \frac{e\hat{F}}{I_o} \frac{1}{\sqrt{\omega^2-\mu^2}} e^{-\mu t} \sin\left(\sqrt{\omega^2-\mu^2}\,t\right) \qquad (39)$$

where

$$\hat{F} = F_m \lambda \quad \#\text{-sec}$$

Since we will compare these results with the previously obtained ones, let us evaluate equation (39) for the values used before:

$$\omega = .314$$

$$\mu = .10$$

$$I_o = 100$$

$$e = 10$$

Hence:

$$\theta_i(t) = .33\hat{F} e^{-\mu t} \sin\left(\sqrt{\omega^2-\mu^2}\,t\right) \qquad (40)$$

which is plotted in figure 14, and is a damped oscillation whose magnitude depends on the impulse $\hat{F}$.

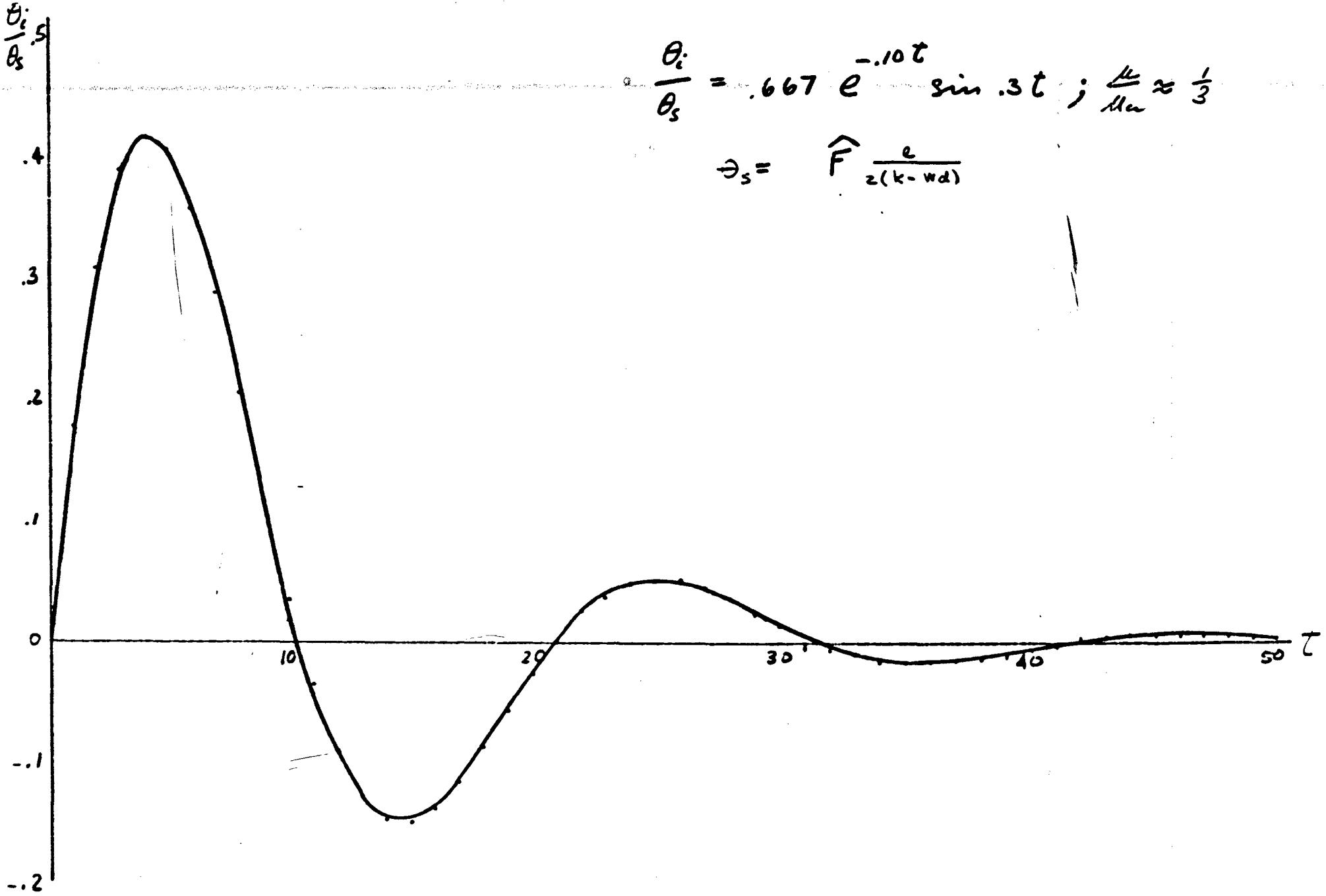

$$\frac{\theta_i}{\theta_s} = .667\, e^{-.10t} \sin .3t \; ; \; \frac{\omega}{\omega_n} \approx \frac{1}{3}$$

$$\theta_s = \hat{F}\,\frac{e}{z(k - wd)}$$

FIG. 14

To investigate the effect of a variation in $\hat{F}$, let us take $F(t)$ as follows:

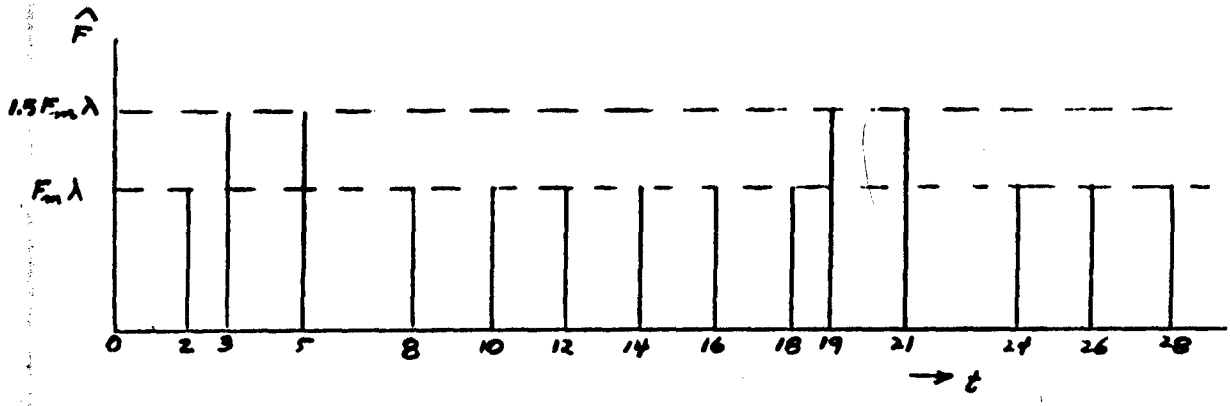

FIG. 15

which is almost periodic except for the occurrence of several pulses of 50% greater amplitude. The system response is evaluated by superposing the responses θ_i to the separate pulses; careful attention being given to the phase due to non-periodic spacing. This has been done and is plotted in Figure 16 where it is compared to the periodic case.

It is seen that irregularities in pulsing can cause sizeable perturbations in the dynamic response of the pendulum. If they occur often enough so that the effect of one has not decayed before another occurs, then getting consistent experimental results may be very difficult.

Additionally, Figure 17 presents the result of a cut-off in the pulses after an "almost" damped displaced position has been attained. From this we see, additionally, that any cut-offs could lead to difficult interpretation of the experiment.

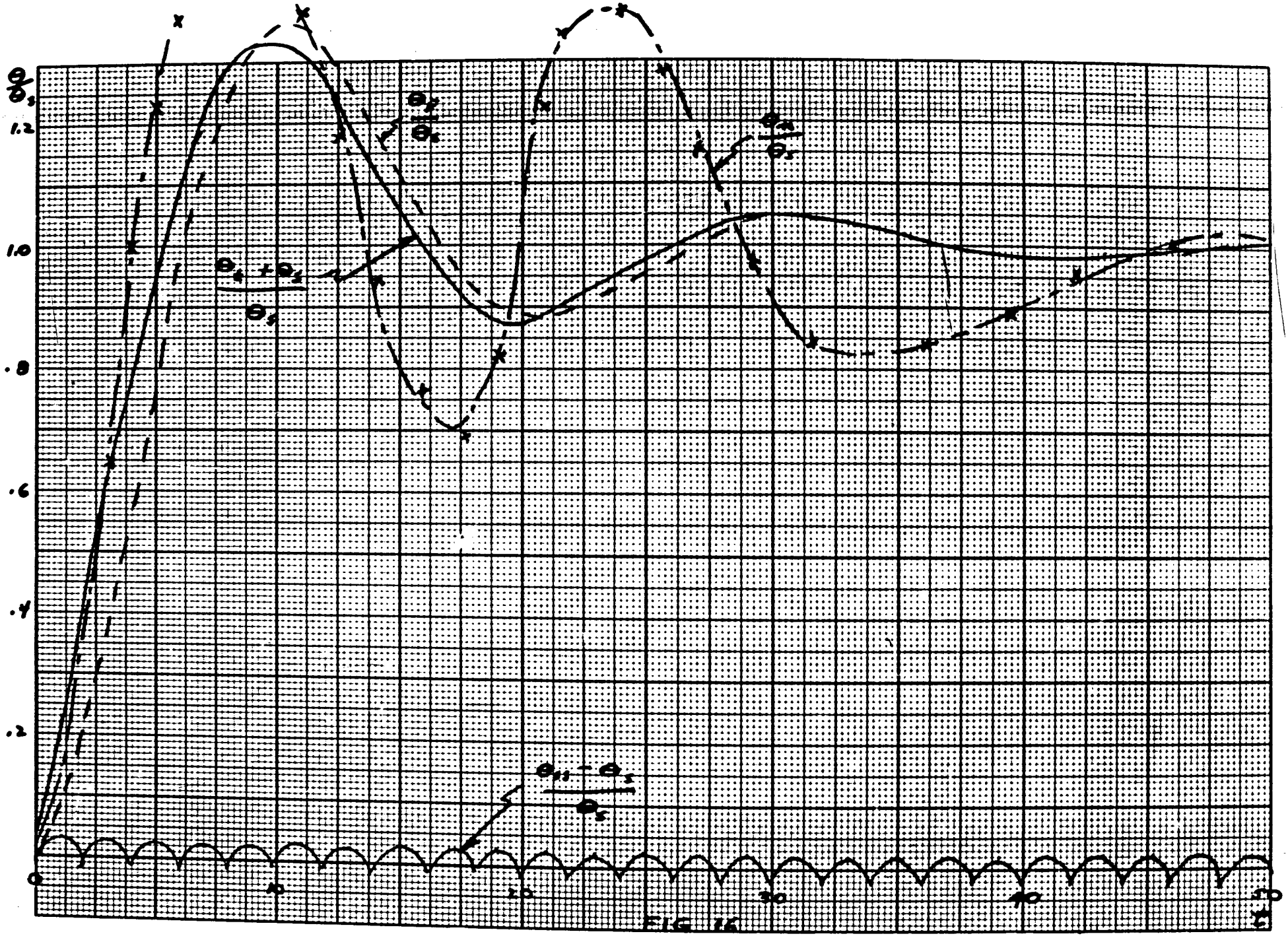

FIG 16

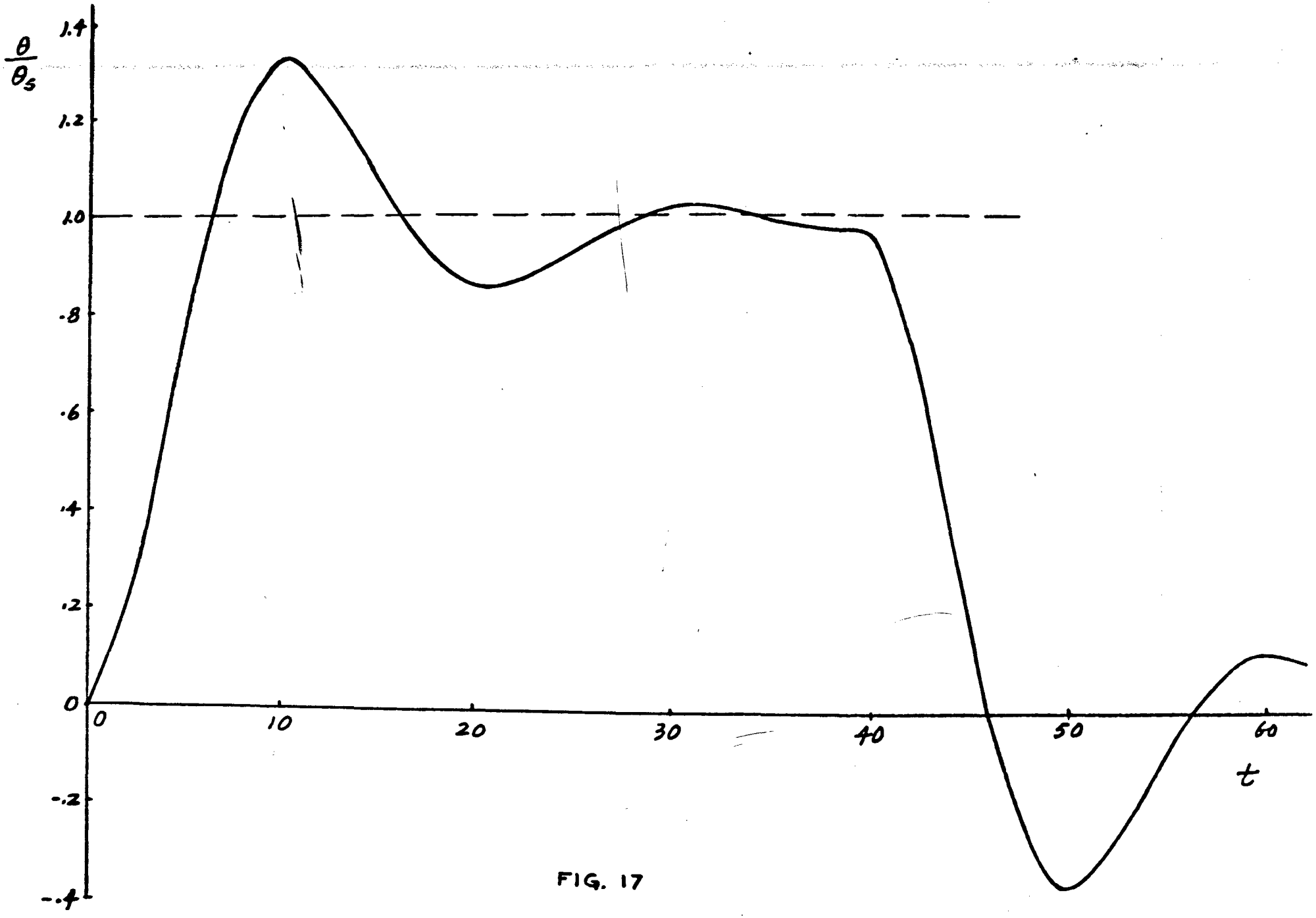

FIG. 17

4. Pivot Buckling Considerations

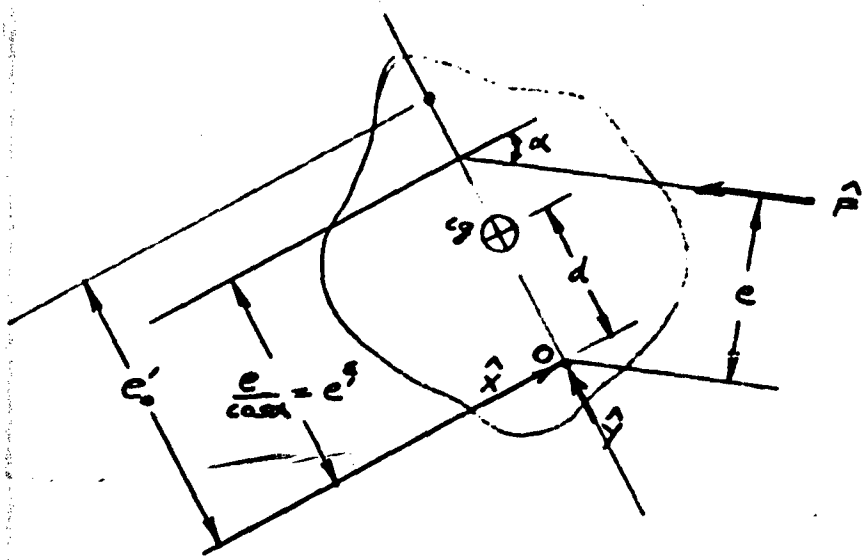

FIG. 18

Consider a rigid body pivoting about point O as shown in Figure 18. An applied impulse $\hat{F}$ results in the reactive impulses $\hat{x}$ and $\hat{y}$ at the pivot. To determine these, write the equations of motion:

$$\begin{aligned} \hat{F}\cos\alpha - \hat{x} &= \frac{W}{g}\Delta\dot{\theta}d \\ \hat{F}\sin\alpha + \hat{y} &= 0 \\ \hat{F}e &= I_o\Delta\dot{\theta} \end{aligned} \qquad (41)$$

where:

$$I_o = I_{cg.} + \frac{W}{g}d^2 \qquad (42)$$

Solving these, we find:

$$\Delta\dot{\theta} = \frac{\hat{F}e}{I_o} \qquad (43)$$

$$\hat{Y} = -\hat{F}\sin\alpha$$

$$\hat{X} = \hat{F}\cos\alpha\left[1 - \frac{Wde}{gI_o\cos\alpha}\right] = \hat{F}\cos\alpha\left[1 - \frac{Wd}{I_o g}e'\right]$$

where e' is the intersection of $\hat{F}$ with the line from the pivot through the center of gravity. Let us define e'_o as the value of e' for which $\hat{X} = 0$; hence:

$$e'_o = \frac{gI_o}{Wd} = d + \frac{gI_g}{Wd} \qquad (44)$$

and

$$\hat{X} = \hat{F}\cos\alpha\left(1 - \frac{e'}{e'_o}\right) \qquad (45)$$

Thus, e'_o defines the center of percussion; if $\hat{F}$ passes through this point ($e' = e'_o$), then $\hat{X} = 0$. If:

$e' < e'_o$ then $\hat{X} > 0$

$e' > e'_o$ then $\hat{X} < 0$

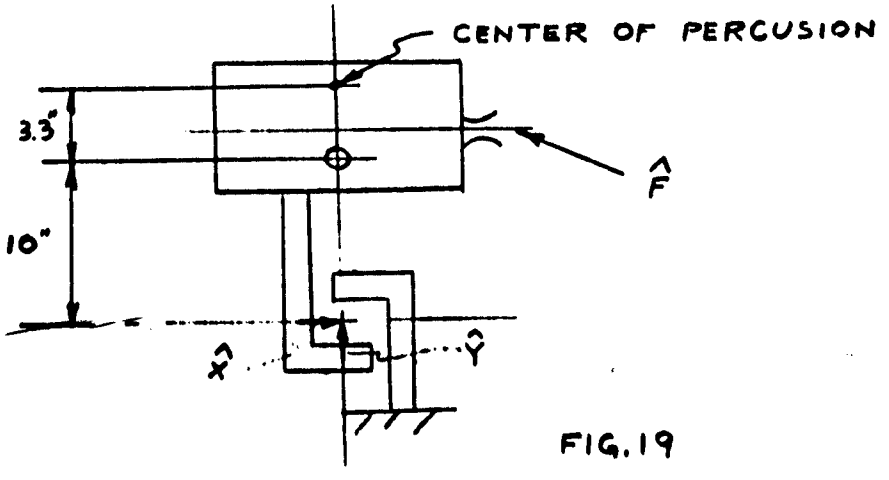

FIG. 19

It has been proposed that the pivot for the inverted pendulum could be obtained with a "Flexure" unit as shown in Figure 19. This unit is composed of thin crossed bands and pivoting is accomplished by their flexing under load. The vertical band is under tension due to the engine weight; the load in the horizontal band depends on the sign of $\hat{X}$. If $\hat{X}$ is positive, then the load in this band is tension; if $\hat{X}$ is negative, then the load will be compressive and may cause a buckling instability. We saw before that if $\hat{F}$ acts below the center of percussion, then $\hat{X} > 0$ Hence, to preclude buckling, it is necessary that $\hat{F}$ act below the center of percussion. The location of the center of percussion is estimated to be about 3.3 inches above the center of gravity; thus, if the line of action of the engine thrust is below this point, the horizontal band will be in tension and perform in a proper manner.

5 - Sources of Erratic Behavior - General Discussion

In order to determine whether the inverted pendulum will provide a reliable, or even measurable, thrust measurement, it is necessary to consider the effects of small departures from ideality. This has been done in a quantitative manner for some non-idealities in the previous sections. Others exist; some of these which seem important will be discussed qualitatively in this section.

a. Ground Motions

It is possible that the very low frequency motions that exist outside of the present equipment, may be transmitted through the pivot and cause unsteady or erratic motion of the engine, even in the absence of the engine thrust. The disturbances which one would be most concerned about are those which have a low frequency component close to that associated with the inverted pendulum system. These low frequency inputs arise from natural ground motions, building vibrations, beating phenomena associated with two or more closely matched inputs, equipment motion, etc. Because of the verylow frequencies involved, if these were troublesome they would be of such a low frequency as to make isolation impractical. Thus, it is necessary that, if these exist, their amplitudes be sufficiently small; even their amplified motions must still have a negligible effect compared to that associated with engine thrust.

The quantitative evaluation of the importance of ground motions on the response of this system still remains; these can be carried out on either an experimental or analytical basis.

b. Other Force Inputs

Because this inverted pendulum integrates and stores the effects of erratic force inputs for a long time duration, it is essential that no others of comparable magnitude to that provided by the engine pulse act on the engine prior to or during the measuring period. As we see

from Figure 16, small extraneous forces or pulses can cause quite large disturbing motions so as to make the experimental results either difficult to obtain and/or to interpret.

Inputs of this nature could arise from the reflected shock waves as the discharged gas bounces around in the vacuum chamber, from the motion of the gas out of the chamber as it is being evacuated, etc. The quantitative effects of these inputs for the design under consideration is beyond the scope of this investigation but they must be carefully evaluated either analytically or experimentally to ascertain that they are negligible and that the measured results are reliable.

B - Stiff System

1. Introduction

We now consider a system of mounting the engine so that its natural frequency is much greater than the pulse frequency; the stiff system.

2. Dynamic Analysis

This system is idealized as follows:

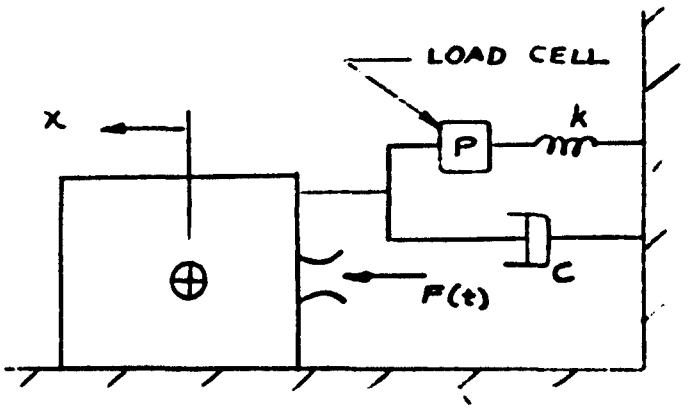

FIG. 20

It is noted that the following equations will be equally valid for a torsional analog to the above system.

The equations of motion are:

$$\ddot{x} + 2\mu\dot{x} + \omega^2 x = \frac{g}{W} F(t) \qquad (46)$$

where

$$2\mu = \frac{cg}{W} \quad ; \quad \omega^2 = \frac{kg}{W}$$

Since we require the system natural frequency much greater than the pulse frequency, and full damping before subsequent pulses, we will investigate the system response to a single pulse. The associated input is shown in the following figure:

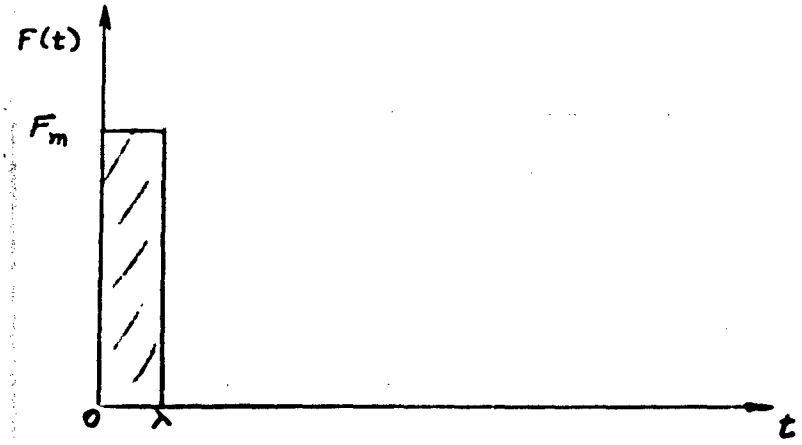

FIG. 21

We find the solution of equation (46) to be:

$$x(t) = \frac{F_m g}{\omega^2 W}\left\{\left[1 - e^{-\mu t}\cos\omega t\right] - \left[1 - e^{-\mu(t'-\lambda)}\cos\omega(t'-\lambda)\right]\right\} \qquad (47)$$

$t' = t$ for $t > \lambda$

$t' - \lambda = 0$ for $t \leq \lambda$

$0 \leq t \leq \infty$

which has the form of a decayed oscillation as follows:

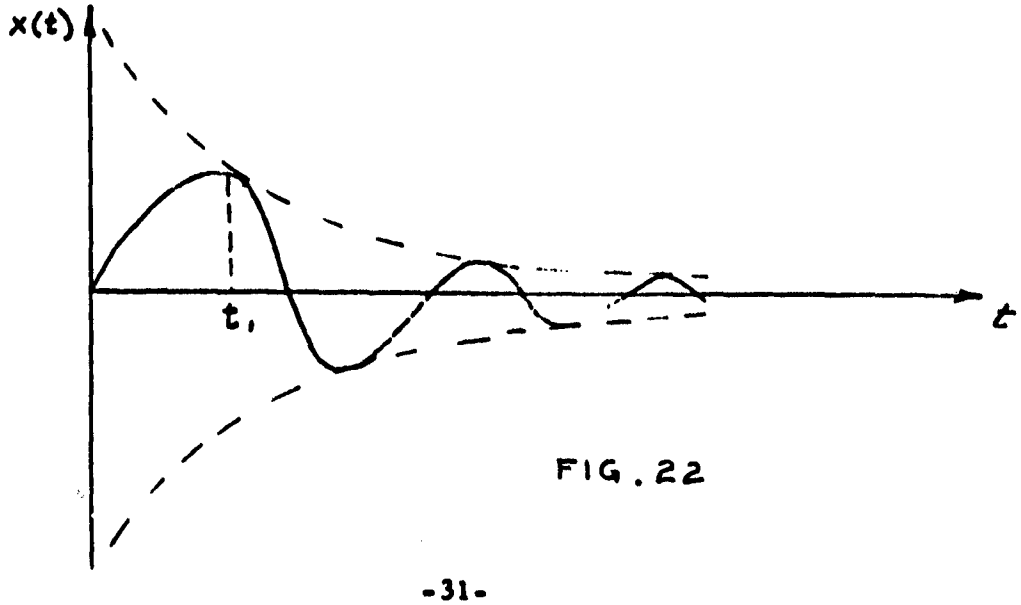

FIG. 22

This will induce a force $(G(t))$ in the load cell which is

$$G(t) = k x(t) \tag{48}$$

Now, it can be shown that, for $t_{max} >> \lambda$, the maximum displacement, and hence the maximum force in the load cell, occurs at:

$$t_1 = \frac{\pi}{2\omega} + \frac{\lambda}{2} \tag{49}$$

Hence, from equation (47) we find

$$G_{max} = G(t_1) = 2\left(\sin\frac{\lambda\omega}{2}\right)F_m \tag{50}$$

$$\approx \lambda\omega F_m \quad \text{for } \frac{\lambda\omega}{2} << 1 \tag{51}$$

Taking: $\omega = 200\pi$ (100 cycle/sec)

$\lambda = .0005$ seconds

$F_m = 20$ pounds

we find the maximum load cell force to be

$$G_{max} \approx 6.3 \text{ pounds}$$

which may be readily measured.

Using a strain measuring device instead of the above described load cell we find, as with the infinitely rigid system, that

$$\varepsilon = \frac{G}{kl} \tag{52}$$

where ℓ is the length of the flexible member.

Introducing equation (52) into (51) we have

$$\varepsilon_{max} \approx \frac{\lambda \omega F_m}{k \ell} \qquad (53)$$

for small $\lambda\omega$. Since $k = M\omega^2$, we have

$$\varepsilon_{max} \approx \frac{\lambda F_m}{\omega \ell \left(\frac{w}{g}\right)} \qquad (54)$$

For the above parameters, taking $\ell \sim .1"$ we have

$$\varepsilon_{max} > 100 \times 10^{-6} \quad in/in \qquad (55)$$

which is readily measured within state-of-the-art techniques.

3. Sources of Erratic Behavior - General Discussion

As with the inverted pendulum system, the reliability of the stiff system is very dependent on the effects of small departures from ideality. The same sources discussed with that application will be considered here.

a- Ground Motion

Only the higher frequency inputs will be able to disturb this system; those of the same order of that described in the above sections. Generally these will be well above those associated with building and ground motions; instead they will come from neighboring equipment. However, in this case because of the degree of natural damping associated

with this system and because of the low amplitude inputs they should not pose a problem. If they do, it will be rather simple to isolate the above discussed system because of the relatively high frequencies under consideration.

b. Other Force Inputs

As with the inverted pendulum these could cause a problem. However, because of its very nature this system records only instantaneous behavior as contrasted to integrated behavior of the inverted pendulum. The result is that only those forces that act almost simultaneously with the pulse could cause trouble. Since the nature of the engine is such that the disturbances from reflected shocks, or gas flow out of the chamber occur after the pulse it is reasonable to expect that they will present no difficulty. Instead it is expected, if they exist, their effect will be as indicated in Figures 23 and 24 below.

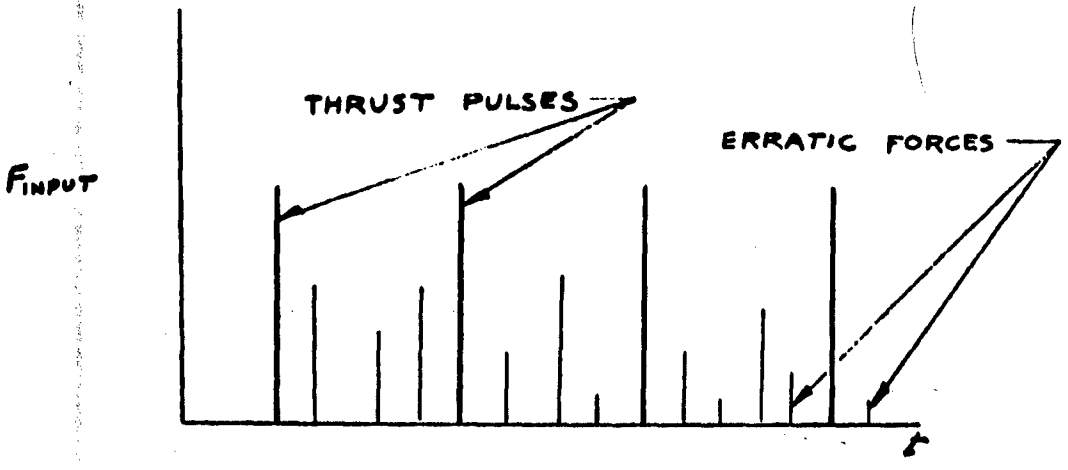

FIG. 23
FORCE INPUT

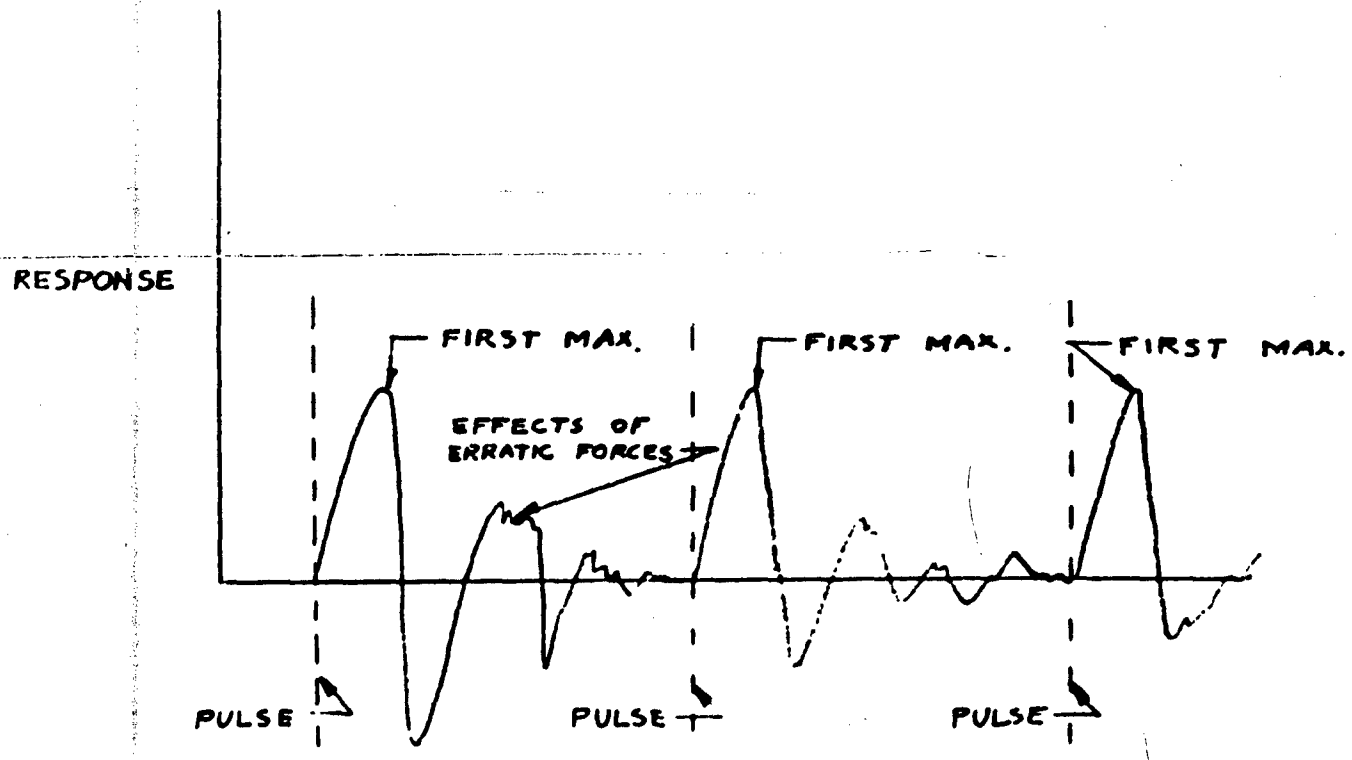

SYSTEM RESPONSE
FIG. 24

In this case we only require a reasonable initial response for the first 1/4 cycle, or approximately 1 to 2 milliseconds, in order to properly interpret and evaluate the engine thrust. This can be compared to the requirement on the inverted pendulum for no erratic forces for at least 10 to 20 seconds.

c. Erratic Thrust Spacing or Magnitude

Whereas this lack of uniformity could cause considerable erratic behavior in the inverted pendulum system, it would be of no concern in the stiff system. This follows because the stiff system responds and measures each pulse separately; so that an erratic pulse history has no effect on capability of this system. Instead, this system should be able to record and evaluate the complete pulse history as it exists.

DISTRIBUTION LIST

Note

Addresses who no longer have a need to receive these reports or who can meet their needs with fewer copies are requested to send the information to:

Chief of Naval Research
Department of the Navy
Washington 25, D.C.
Attention: Power Branch (Code 429)

AGENCY	No. of Copies
Chief of Staff U.S. Air Force, The Pentagon Washington 25, D.C. Attention: DCS/D, AFDRD-AN/PO DCS/D, AFDRD-EX	 1 1
Commander Air Force Ballistic Missiles Division P.O. Box 262 Inglewood, California (Attention WDSOT)	1
Commander Air Force Cambridge Research Center, ARDC Bedford, Massachusetts Attention: CROOTR	1
Commander Air Force Missile Test Center Patrick Air Force Base, Florida Attention: Technical Information and Intelligence Branch (MTGRY)	1
Air Force Office of Scientific Research Temporary T Building Washington 25, D.C. Attention: SREC	1
Commander Air Research and Development Command Andrews Air Force Base Washington 25, D.C. Attention: RDSBTL	2

DISTRIBUTION (Cont'd)

AGENCY	No. of Copies
Director Air University Library Maxwell Air Force Base, Alabama	1
Commander-in-Chief Strategic Air Command Offutt Air Force Base, Nebraska Attention: Director of Operations Missile Division	1
Commanding General Antiaircraft Artillery and Guided Missiles Center Fort Bliss, Texas	1
Director, Project Rand Department of the Air Force 1700 Main Street Santa Monica, California	1
Chief, Document Service Center Armed Services Technical Information Agency Arlington 12, Virginia	10
Director, Operations Research Office Department of the Army 6935 Arlington Road Bethesda, Maryland Attention: Library	1
Commanding General Army Ballistic Missile Agency Redstone Arsenal, Alabama Attention: Technical Documents Library	1
Commanding General Engineer Research and Development Laboratories U.S. Army Fort Belvoir, Virginia	1
Commander Army Rocket and Guided Missile Agency Redstone Arsenal, Alabama Attention: Technical Library	1
U.S. Atomic Energy Commission Los Alamos Scientific Laboratory P.O. Box 1663 Los Alamos, New Mexico Attention: Miss Helen Redman	1

DISTRIBUTION (Cont'd)

AGENCY	No. of Copies
U.S. Atomic Energy Commission Technical Information Services Extension P.O. Box 62 Oak Ridge, Tennessee	1
U.S. Atomic Energy Commission Sandia Corporation P.O. Box 5400 Albuquerque, New Mexico	1
U.S. Atomic Energy Commission Sandia Corporation, Livermore Branch P.O. Box 969, Livermore, California Attention: Mr. James McMinn Document Control Section	1
U.S. Atomic Energy Commission University of California Radiation Laboratory Technical Information Division P.O. Box 808 Livermore, California Attention: Clovis Craig	1
Commander, Holloman Air Development Center Holloman Air Force Base, New Mexico Attention: Technical Library (HDOI)	1
Commanding Officer Naval Air Development Center Johnsville, Pennsylvania	1
Commander U.S. Naval Air Missile Test Center Point Mugu, California	1
Commanding Officer Naval Ordnance Laboratory Corona, California Attention: Documents Library	1
Commander Naval Ordnance Laboratory White Oak, Silver Spring 19, Maryland Attention: The Library, Room 1-333	1

DISTRIBUTION (Cont'd)

AGENCY	No. of Copies
Commander, U.S. Naval Ordnance Test Station China Lake, California Attention: Technical Library	1
Superintendent U.S. Naval Postgraduate School Monterey, California	1
Chief of Naval Operations (OP-51) Department of the Navy Washington 25, D.C.	1
Chief of Naval Operations Department of the Navy Washington 25, D.C. Attention: OP-34, OP-37, OP-03EG	3
Chief, Bureau of Naval Weapons Department of the Navy Washington 25, D.C.	
Attention: RAPP	1
RMMP	1
Director, U.S. Naval Research Laboratory Washington 25, D.C. Attention: Code 2027	1
Commanding Officer Office of Naval Research The John Crerer Library Building 86 East Randolph Street Chicago 1, Illinois	1
Commanding Officer Office of Naval Research Branch Office 346 Broadway New York 13, New York	1
Commanding Officer Office of Naval Research Branch Office Navy No. 100 Fleet Post Office New York, New York	2
Commanding Officer Office of Naval Research Branch Office 1030 East Green Street Pasadena 1, California	1

DISTRIBUTION (Cont'd)

AGENCY	No. of Copies
Office of Naval Research Department of the Navy Washington 25, D.C. Attention: Code 429	5
Code 419	1
Office of the Assistant Secretary of Defense for Research and Engineering Room 3E1065, The Pentagon Washington 25, D.C. Attention: Technical Library	1
Director of Weapons Systems Evaluation Group Office of the Assistant Secretary of Defense for Research and Engineering Room 2E1006, The Pentagon Washington 25, D.C.	1
Director of Guided Missiles Office of the Secretary of Defense Room 3C-131, The Pentagon Washington 25, D.C.	1
Central Intelligence Agency 2430 E Street N.W. Washington 25, D.C. Attention: OCR Mail Room	2
Office of Technical Services Department of Commerce 14th and Constitution Avenue Washington 25, D.C.	1 (Unclass. only)
Commanding Officer Diamond Ordnance Fuze Laboratories Washington 25, D.C. Attention: ORD-TL-06.33	1
Jet Propulsion Laboratory 4800 Oak Grove Drive Pasadena, California Attention: Library	1

DISTRIBUTION (Cont'd)

AGENCY	No. of Copies
Commanding Officer, Office of Ordnance Research Box CM, Duke Station Durham, North Carolina Attention: ORDOR-PC	1
Director, National Security Agency Washington 25, D.C. Attention: CREF-22	1
Commanding General White Sands Missile Range, New Mexico Attention: ORDBS-OM-Technical Library	1
Commander, Air Technical Intelligence Center Wright-Patterson Air Force Base, Ohio Attention: AFOIN-4B1a	1
Commander, Wright Air Development Center Wright-Patterson Air Force Base, Ohio Attention: WCOSI-3	5
Commander, Detachment 1, ARDC Wright-Patterson Air Force Base, Ohio Attention: RDZS	1
Aerojet-General Corporation Azusa, California Attention: Mr. M.T. Grenier	1
Aero-jet General Corporation Liquid Rocket Plant P.O. Box 1947 Sacramento 9, California Attention: Miriam S. Nylin, Librarian	1
Applied Physics Laboratory The Johns Hopkins University 8621 Georgia Avenue Silver Spring, Maryland Attention: Mr. G.L. Seielstad	1
Bell Aircraft Corporation P.O. Box 1 Buffalo 5, New York Attention: Mrs. Eunice P. Hazelton	1

DISTRIBUTION (Cont'd)

AGENCY	No. of Copies
Boeing Airplane Company Pilotless Aircraft Division P.O. Box 3707 Seattle 24, Washington Attention: R.R. Barber, Library	1
Chance Vought Aircraft, Inc. P.O. Box 5907 Dallas, Texas Attention: Mr. P.C. Moran	1
Chrysler Corporation, Missile Operations P.O. Box 2628 Detroit 31, Michigan Attention: Technical Library	1
Convair A Division of General Dynamics Corporation Fort Worth 1, Texas Attention: Mr. K.G. Brown, Engineering	1
Convair A Division of General Dynamics Corporation, Pomona Division P.O. Box 1011 Pomona, California Attention: Mr. C.F. Bradley, Engineering Librarian	1
Convair - Astronautics A Division of General Dynamics Corporation 5001 Kearney Villa Road San Diego 11, California	1
Cornell Aeronautical Laboratory Buffalo, New York Attention: Miss Elma T. Evans, Librarian	1
Curtiss-Wright Corporation Research Division Quehanna, Pennsylvania Attention: Mr. Thomas Minder	1
Douglas Aircraft Company 300 Ocean Park Boulevard Santa Monica, California Attention: Mr. R.L. Johnson, Chief Engineer Missiles and Space Systems	1

DISTRIBUTION (Cont'd)

AGENCY	No. of Copies
Experiment Incorporated P.O. Box T Richmond 2, Virginia Attention: Elaine S. Weil, Librarian	1
General Electric Company Aircraft Gas Turbine Division Central Library, Building 305 Cincinnati, Ohio Attention: Mr. J. J. Brady	1
Giannini Research Laboratory 18400 South Main Street Santa Ana, California Attention: Josephine K. Hagele, Librarian	1
Goodyear Aircraft Corporation Akron 15, Ohio Attention: Mr. E.A. Brittenham, Jr.	1
Grumman Aircraft Engineering Corporation Bethpage, Long Island, New York Attention: Mr. Robert Nafis	1
Hughes Aircraft Company Florence Avenue at Teal Street Culver City, California Attention: Mrs. Audrey M. Diver	1
Lockheed Aircraft Corporation Missile Systems Division P.O. Box 504 Sunnyvale, California	1
Marquardt Aircraft Company 16555 Saticoy Street P.O. Box 2013 South Annex Van Nuys, California Attention: R.E. Marquardt	1
The Martin Company, Denver Division P.O. Box 179 Denver 1, Colorado Attention: Mr. Jack M. McCormick, Research Library	1

DISTRIBUTION (Cont'd)

AGENCY	No. of Copies
McDonnell Aircraft Corporation P.O. Box 516 St. Louis 3, Missouri Attention: Dr. B.G. Bromberg	1
North American Aviation, Inc. Missile Development Division 12214 Lakewood Boulevard Downey, California Attention: Engineering Library, 495-115	1
Northrop Corporation Norair Division 1001 E. Broadway Hawthorne, California Attention: Technical Information	1
Princeton University Forrestal Research Center Library Project SQUID Princeton, New Jersey Attention: Mr. M.H. Smith	1
Purdue University Lafayette, Indiana Attention: Dr. M. J. Zucrow	1
Raytheon Manufacturing Company Missiles Systems Division Bristol, Tennessee Attention: Mr. G. Longnecker	1
Reaction Motors, Inc. Division of Thiokol Chemical Corporation Ford Road Denville 1, New Jersey Attention: Mrs. Margaret Becker	1
Rocketdyne Division of North American Aviation, Inc. 6633 Canoga Avenue Canoga Park, California Attention: Mr. Thomas F. Dixon	1

DISTRIBUTION (Cont'd)

AGENCY	No. of Copies
Ryan Aeronautical Company Lindbergh Field San Diego 12, California Attention: Stella Derkson	1
Stanford Research Institute Documents Center Menlo Park, California Attention: Mary Lou Fields, Acquisitions	1
United Aircraft Corporation Research Department East Hartford 8, Connecticut Attention: Mr. C.H. King	1
Vitro Laboratories Division of Vitro Corporation of America 14000 Georgia Avenue Silver Spring, Maryland Attention: Miss C. Marion Jaques	1
Wiancko Aeronautics 255 North Halstead Avenue Pasadena, California	1